Reduced Graphene Oxide Synthesis via Improved Hummers' Method

[*1]Rafig Alibeyli, [1]Ali Ata and [**1]Erdal Topaç
[1]Gebze Institute of Technology, Nanotechnology Research Center, Gebze - Kocaeli

Abstract

In this study, we focused on production of RGO[1] by reduction of GO[2]. GO was obtained via an improved Hummers' method. Chemical reduction of GO with hydrazine and with sodium borohydride were conducted. Effects of the used reduction procedures on RGOs' properties were investigated. Consequently, an easily controllable procedure was reached and several RGO gradients were synthesized. The synthesized RGO samples were investigated by XRD, SEM, EDAX, FTIR, TGA, BET and Raman spectroscopy. Crystallographic structure, morphologic appearance, and elemental ingredients of RGOs' were identified. Nearly 9,5:1 C:O ratio was reached . Using the resulted RGO as anode support material in lithium ion battery is planned to improve batteries charge capacity.

Key words: Graphene Oxide, Reduced Graphene Oxide, Hummers' Method, Lithium Ion Battery, Anode Support Material.

[1] Reduced Graphene Oxide
[2] Graphene Oxide

*Corresponding author: Address: Nano Technology Research Center Gebze Institute of Technology Cayirova Kampusu, 41400, Gebze/Kocaeli, TURKEY. E-mail address: rafig.alibeyli@yahoo.com, Phone: +905356135255

**Corresponding author: Address: Nano Technology Research Center Gebze Institute of Technology Cayirova Kampusu, 41400, Gebze/Kocaeli, TURKEY. E-mail address: erdaltopac@hotmail.com, Phone: +905355837240

1. Introduction

An effective production and storage of electricity is a key issue to meet the ever raising energy demand. Lithium ion batteries as a remarking energy source and graphene derivatives as anode support material are promising selections as battery components. [1]

Graphene is a fascinating novel material with its high specific surface area (theoretically 2630 m^2/g), extraordinary electronic and optic properties and electron transport capabilities, excellent thermal and electrical conductivities and strong mechanical strength. One of the allotropes of elemental carbon, graphene, is a planar monolayer of carbon atoms arranged into a two-dimensional (2D) honeycomb lattice with a carbon–carbon bond length of 0.142 nm [2] Electrons in graphene behave like massless relativistic particles, which contribute to very peculiar properties such as an anomalous quantum Hall effect and the absence of localization [3,4]. Graphene [3] has demonstrated a variety of intriguing properties including high electron mobility at room temperature (250,000 cm^2/Vs) [5,6] exceptional thermal conductivity (5000Wm^{-1} K^{-1}) [7] and superior mechanical properties with Young's modulus of 1 TPa [8]. Its potential applications include single molecule gas detection, transparent conducting electrodes, composites and energy storage devices such as supercapacitors and lithium ion batteries [8-21].

Graphene derived from natural graphite by such methods that mechanical exfoliation, liquid phase exfoliation or reduction of graphene oxide (e.g.) generally. Graphene Oxide (GO) and the following stage Reduced Graphene Oxide (RGO) is one of precursors of Graphene synthesis. The Hummers' method is one of the prominent methods for synthesizing graphene oxide. After elimination of the functional oxygen containing groups, RGO is obtained. The elimination (reduction of GO) can be conducted by chemical, thermal, solvothermal or microwave initiated routes etc.

In this study, we focused on production of RGO by reduction of GO obtained via an improved Hummers' method. Using the resulted RGO as anode support material in lithium ion battery is planned to improve batteries charge capacities.

2. Materials and Method

The used chemicals are natural graphite flakes (Kropfmühl-Graphite V-Cond 8/99,9), $NaNO_3$ (pure 98%), H_2SO_4 (95-98%),$KMnO_4$ (99%) HCl (37% Honeywell), $BaCl_2$ (5% aqueous solution), $AgNO_3$ (1,7% aqueous solution), $NaBH_4$, Hydrazine hydrate (reagent grade, N_2H_4 50-60 % Sigma Aldrich) are used for RGO synthesis via improved Hummers' method.

Nüve NF1200 centrifuge was used for centrifugation. Philips XL 30 SFEG was used for SEM imaging EDAX detector was used for elemental analysis. Rigaku RINT 2200 XRD was used to determine crystallographic structure. Tecnai G2 F20 S-TWIN was used for TEM and STEM imaging. FT-IR Perkin Elmer 100 was used for identification of functional groups. Mettler Toledo thermal analysis system TGA/SDTA 851 was used for thermogravimetric analysis. Thermo Scientific DXR Raman microscope was used for identification of layer numbers.

2.1. Synthesis of GO

Graphene oxide was prepared by improved Hummers method. In a typical preparation, 5 g $NaNO_3$ was added to cold H_2SO_4 solution (230 ml, 95-98%) prepared at 7 °C in an ice bath and stirred by a magnetic stirrer for 5 minutes. Then, 5 g natural graphite flakes were added to this beaker and stirred by a magnetic stirrer for 5 minutes and then 25 g KMnO4 added to the baker slowly in 15 minutes. During the addition, suspension's temperature was kept below 15°C. Once mixed, the suspension was transferred to a 35 ± 5 °C water bath and stirred for about 1 h, forming a thick paste. Then, 400 ml ultrapure water was added to the reaction beaker. When the ultrapure water was added, the temperature has raised up to 90 °C. At this stage, the temperature was kept at 90±5°C. The suspension was stirred for extra 30 minutes at this temperature. Finally, 1000 mL of water containing 60 mL of H_2O_2 was added to the suspension. The color of the suspension was turned from dark brown to yellow. High concentrated HCl was added to the final suspension to accelerate precipitation. The solid content of final suspension was precipitated by centrifugation with 9000rpm in 5 minutes. After that, for purifying from SO_4^{2-} , the precipitants was dispersed in HCl (3.7%) and stirred for 15 minutes. Then, the centrifugation was applied again at 9000rpm. This treatment was repeated until SO_4^{2-} was not indicated by $BaCl_2$. Then, in order to purify Cl^- ions, precipitants that purified from $SO4^{2-}$ was dispersed in pure water. The suspension was stirred for 15 minutes by magnetic stirrer and then centrifuged at the same conditions. The final precipitant was dried in an oven at 40-80°C temperature under vacuum and grinded.

2.2. Reduction of GO

GO reduced by hydrazine monohydrate and by $NaBH_4$. In a typical reduction GO (0,6gr) was stirred mechanically in 200 ml pure water and was dispersed finely in water by ultrasonic bath for three hours. Then, while the GO suspensions were stirred $NaBH_4$ (2 gr) or hydrazine monohydrate (0,25ml) was added to the GO suspension. The suspension was heated by autoclave or hot plate. The solution was heated in an oil bath at 80-100 °C under a water-cooled condenser or without condenser for 12 and 24 h. Water level was kept during all the reductions. RGO's were precipitated by centrifugation or filtration. Then, precipitated RGO samples were washed with acetone and pure water and ethanol. Finally, washed and precipitated RGOs were dried in an oven with or without vacuum.

3. Results

3.1. Synthesized GO

Different experimental studies were conducted to reach optimum conditions for GO synthesis. In this work, the main objective is to obtain GO with high oxidation ratios, low impurities, fewer layer numbers and higher efficiency. The results of selected experimental studies (ETGO05, ETGO07A, ETGO08, ETGO8Ç, ETGO09-1, ETGO09-2, ETGO09-3, ETGO10, and ETGO11) were investigated and interpreted:

Dehydration process was performed by the filtration or drying of GO samples in an oven until the experiment ETGO05. Then in following synthesis, the process was replaced by mixing and

heating on a hot plate at 50±5 °C. Additionally, washing times were extended. Centrifugation rpm's were raised from 8000rpm up to 9000-10000 rpm. Until experiment ETGO07, we could not reach 90 °C while ultrapure water was added. During following experiments, it was reached 90 °C by heating on a hotplate or spontaneously. Suspensions were mixed at this temperature during 30 minutes. Until experiment ETGO08 bigger GO particles were eliminated by low rpm centrifugation. According to XRD results, we have seen no difference between the main product of our reaction and the eliminated bigger particles. Thus, the low rpm centrifugation was cancelled, which increased the efficiency of the synthesis.

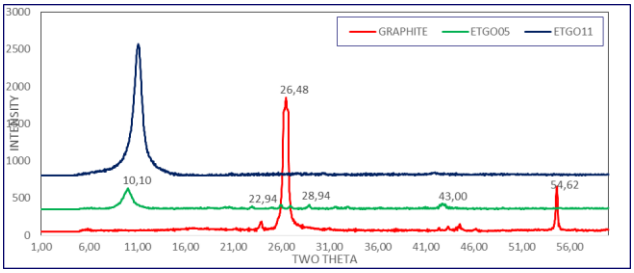

Figure 1. X Ray diffraction patterns of synthesized graphite and GO samples [Graphite, ETGO05, ETGO11]

XRD patterns of GO for selected synthesis are given in Fig. 1. Both of the samples show characteristic GO peaks between 2θ=9-11°. It was clearly seen that changing the washing and precipitation conditions reduced the amounts of impurities.

The C:O ratios of selected GO samples derived from EDAX analysis are given in Table 1. The oxidation degree of GO was calculated by using C:O ratios of samples. Among these experiments, the lowest C:O ratio was acquired for ETGO10 as seen in Table 1. This result was indicated as the highest oxidation degree in our experimental study.

Table 1. Atomic C/O ratios of ETGO08, ETGO08Ç, ETGO09-3, and ETGO11

Atomic %	ETGO08	ETGO08Ç	ETGO09-3	ETGO10	ETGO11
C	69,25	70,98	65,81	60,85	62,62
O	27,24	25,12	31,62	39,15	35,02
C/O	2,54	2,83	2,08	1,55	1,79

Morphological appearances of GO samples obtained from SEM images were given in Fig. 2.

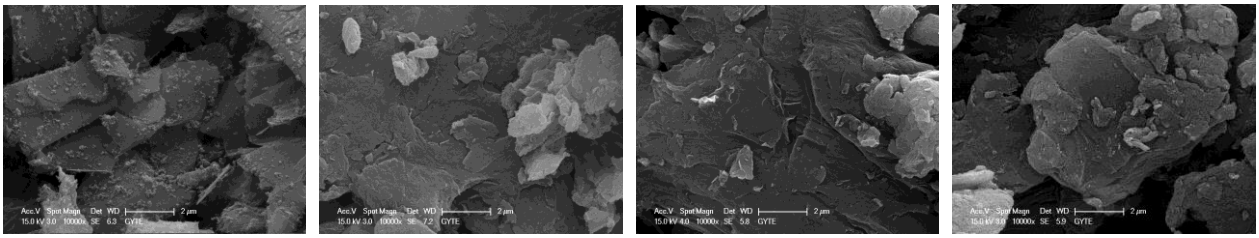

Graphite (2µm) ETGO08 (2µm) ETGO09-3(2µm) ETGO11 (2µm)

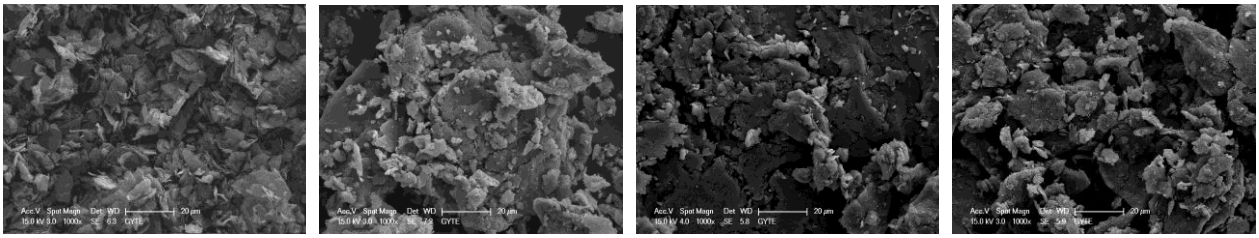

Graphite (20µm) ETGO08 (20µm) ETGO09-3(20µm) ETGO11 (20µm)

Figure 2. SEM Images of Graphite, ETGO08, ETGO09-3, ETGO11, with 2 and 20 µm scale

As seen from SEM images, the morphological appearance of GO samples were altered with synthesis conditions. This is an indication of the applied procedures which effects both the oxidation degree and the morphological structure.

It was assumed that various functional groups including oxygen were tied on GO flakes during oxidation of graphite by Hummers' method. These functional structures are hydroxyl and epoxy groups on the basal plane, with a smaller amounts of carboxy, carbonyl at the sheet edges.

As seen Fig.3-A C=O stretching vibration peak at 1721 cm $^{-1}$, the vibration and deformation peaks of O–H groups at 3391 cm $^{-1}$ and 1410 cm $^{-1}$, respectively, the C–O stretching vibration peak at 1221 cm^{-1}, the C–O (alkoxy) stretching peak at 1046 cm$^{-1,}$ Alkenyl C=C stretching peak at 1680 - 1620 cm $^{-1}$ [46] observed on FT-IR spectrum.

In the infrared spectra, increasing intensities of characteristic peaks of functional groups revealed that the oxidation degree of resulted GO samples increased. The highest peak intensity of functional groups were observed for ETGO10 and ETGO11 GO samples. This fact is compatible with low C:O ratio defined by EDAX analysis.

Although GO is thermally unstable and starts to lose mass upon heating even below 100 °C , the major mass loss occurs at 200 °C, presumably due to pyrolysis of the labile oxygen-containing functional groups, yielding CO,CO_2, and steam. Hence, the thermal decomposition of GO can be accompanied by a vigorous release of gas, resulting in a rapid thermal expansion of the material. This is evident by both a large volume expansion and a larger mass loss. (Fig. 3-B)

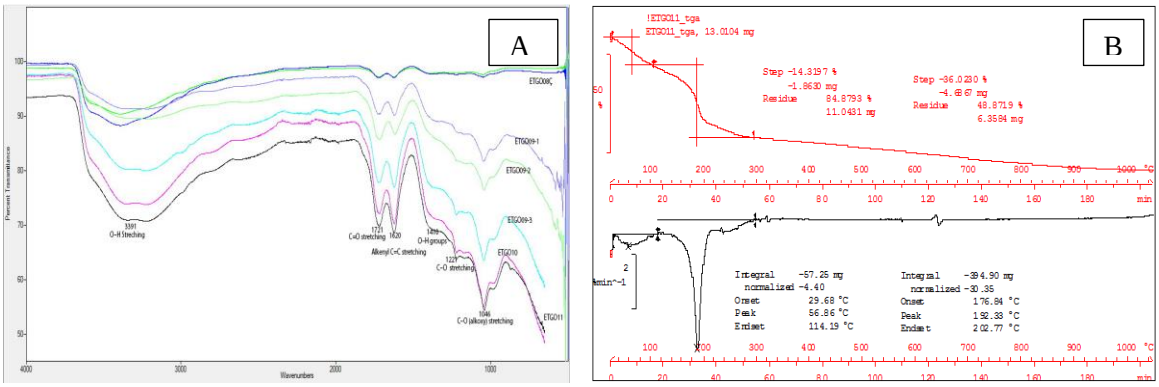

Figure 3. A) FT-IR spectrum of selected synthesized GO samples ETGO [08-11]. **B)** TGA of ETGO11

The definition of layer numbers of obtained GO samples were performed by RAMAN, AFM, and TEM analysis. In this work, the same methods were used to determine the layer numbers of GO samples. Selected RAMAN DXR spectra of GO samples are given in Fig. 4-A. D peaks (1340 cm-1), G peaks (1590 cm-1), and 2D peaks (2700 cm-1) were indicated in Fig. 4-A. Generally, it is assumed that there is a correlation between layer numbers of GO and (G/ 2D) peaks intensities ratios. (G/2D) ratio of ETGO11 was determined about 2.4.

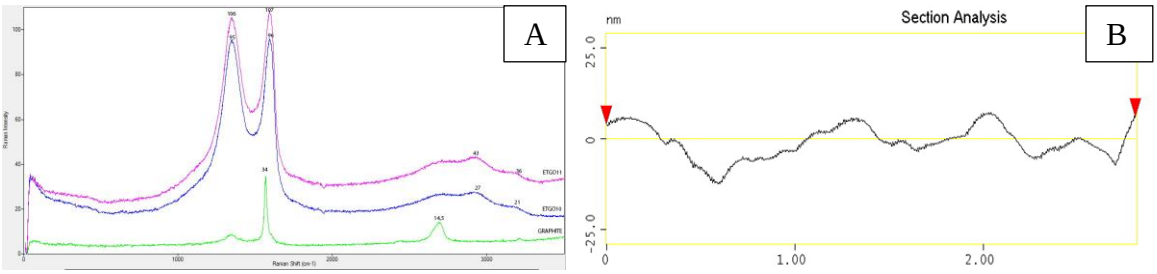

Figure 4. A)Graphite, ETGO10, ETGO11 Raman DXR Spectrums. B) AFM height profile of ETGO11.

AFM analysis that done for definition of layer numbers of ETGO11 sample is shown on Fig. 4-B. According to height profile that obtained AFM analysis, vertical distance of scanned direction is 1,88nm. Distance between graphene layers known as 3,35 °A. Thus, it can be concluded that ETGO11 has nearly six layers. Specific surface area for ETGO11 is obtained from BET analysis as 136.3 m^2/gr. TEM images of ETGO11 are shown on Fig.5

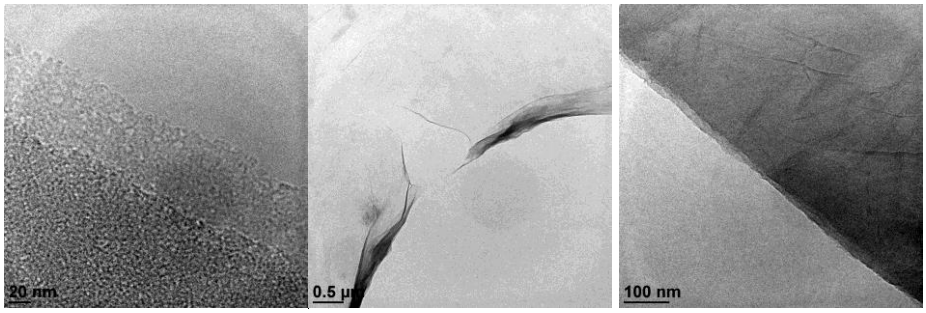

Fig. 5 TEM images of ETGO11

3.2. Synthesized RGO

ETRGO01 obtained from reduction of ETGO11 by $NaBH_4$ and ETRGO03, ETRGO04, ETRGO05 and ETRGO06 were obtained from reduction of ETGO11 by hydrazine monohydrate under differing conditions. X ray diffraction patterns of above mentioned samples are given below (Fig. 6)

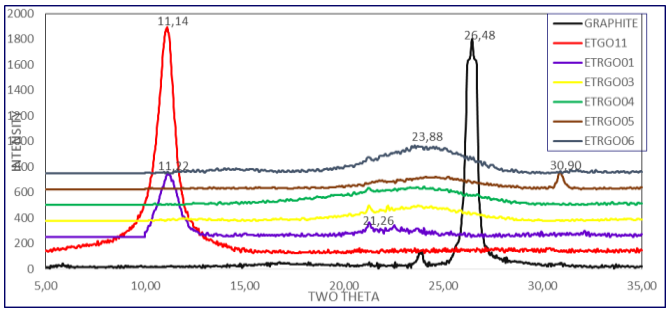

Figure 6. XRD diffraction patterns of graphite, ETGO11, ETRGO [01, 03-06]

One of important characteristic features of RGO is its C: O atomic ratio. C:O ratios of reduced graphene oxide samples were derived from EDAX analysis and listed below (Table. 2). Among these, highest C:O atomic ratio is belong to ETRGO04

Table 2. C:O ratios of ETRGO [01, 03-06] derived from EDAX.

Experiment	Atomic C %	Atomic O %	C:O
ETRGO01	96,47	21,74	4,44
ETRGO03	53,32	7,67	6,95
ETRGO04	88,6	9,36	9,47
ETRGO05	76,51	9,63	7,94
ETRGO06	72,73	16,86	4,31

SEM images of ETGO11 and RGOs obtained from reduction of ETGO11 (Fig. 7)

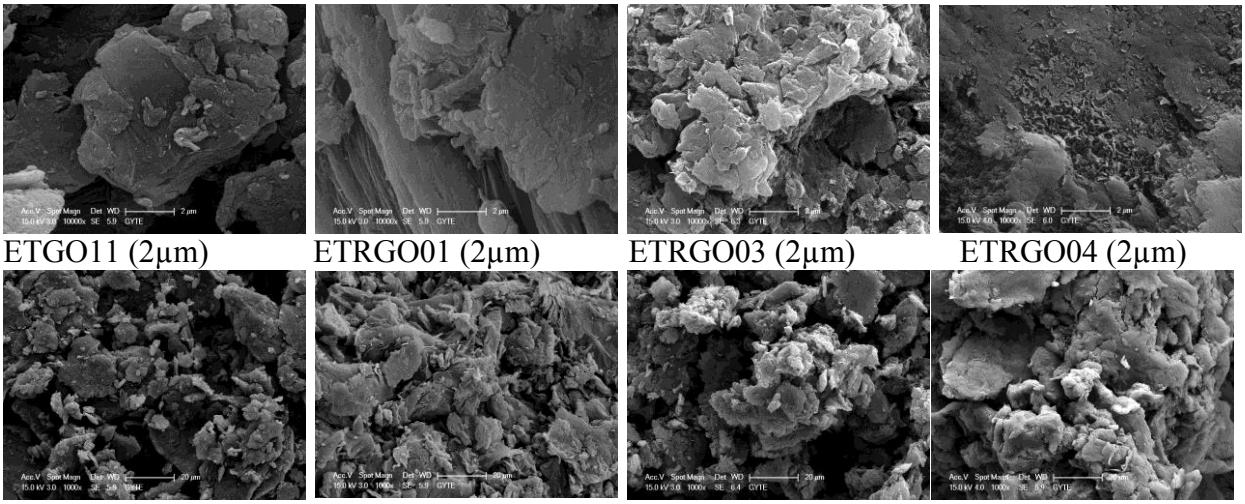

Figure 7. SEM Images ETGO11, ETRGO [01, 03, 04]

FT-IR spectrums show that functional groups tied on GO were eliminated by reduction. (Fig. 8-A). FT-IR spectrum of ETRGO11 are given for comparison. DXR Raman spectrums of ETRGO04 and ETRGO05 are given on Fig. 9. It is obvious that, G peak intensity of ETRGO04 sample is smaller than ETRGO05 samples G peak. There is no attractive difference between 2D peaks of the two samples.

The removal of the thermally labile oxygen functional groups by chemical reduction results in much increased thermal stability for the reduced GO. Apart from a slight mass loss below 100 °C, which can be attributed to the loss of adsorbed water, no significant mass loss is detected when this material is heated up to 1000 °C. (Fig. 8-B)

Specific surface area for ETRGO05 is obtained from BET analysis as 657.46 $m^{2/}$gr.

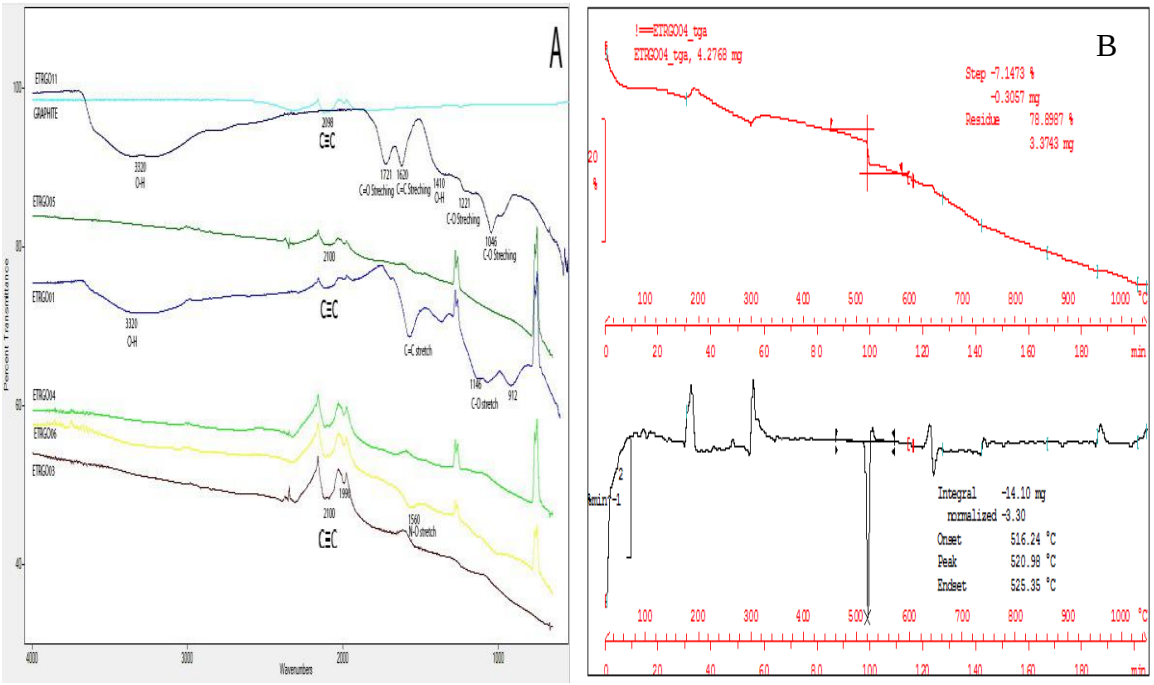

Figure 8. A) FT-IR spectrum of selected synthesized GO samples **B)** TGA of ETRGO04

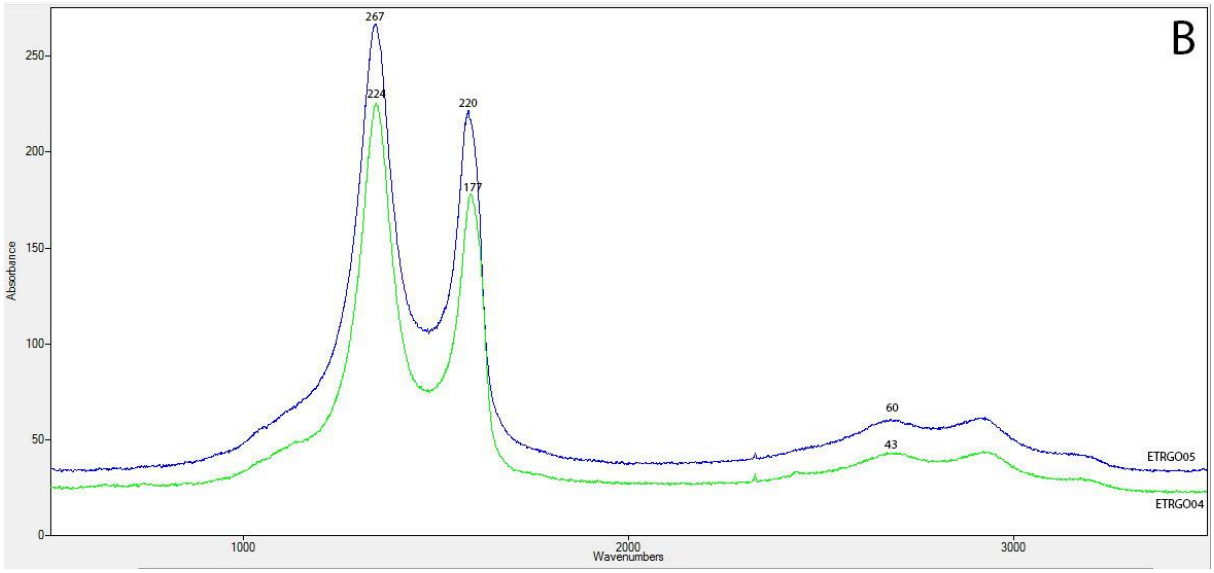

Figure 9. Raman DXR Spectrums of ETRGO04 and ETRGO05

4. Discussion

The characteristic peak of GO around 2θ=11° absent all of the samples except ETRGO01.

This indicated that for our experimental conditions reduction by $NaBH_4$ is not satisfying. Reduced samples X-ray diffraction patterns show necks around 2θ= 23-27 °. Neck has highest intensity belongs to ETRGO06. It is concluded that reductions were successful except ETRGO01 threated with $NaBH_4$ .The C:O characteristic of ETRGO04 is the highest result reached in this work. It is thought that keeping water level of GO suspension while heating on a hot plate promotes GOs reduction degrees. Morphological appearances alter with experimental conditions. (Fig. 7) FT-IR spectras support X-ray diffraction patterns and indicate that $NaBH_4$ is not a successive reducing agent for these experimental conditions. Presence of O-H and C-O functional groups on ETRGO01 FT-IR spectrogram prove the conviction. It is proved that the functional groups eliminated for hydrazine reduced samples. G peak intensity of ETRGO04 smaller than ETRGO05's G peak, this indicates that ETRGO04 has less layer number compared to ETRGO05.Specific surface area of ETRGO05 four times bigger than ETGO11. Then it is expected that ETRGO04 has fewer layer than ETGO11. Consequently, the layer number of ETGO04 should be less than six layers.

Conclusions

Reduction of GO synthesized via improved Hummers' method was investigated under different conditions. Results show that hydrazine monohydrate is a more effective reductant than $NaBH_4$ for our experimental conditions. Highest reduction ratio was reached for ETRGO04 (C:O = 9,5 atomically). Functional groups like C-OH, C=O are not detected on samples reduced by hydrazine monohydrate. Specific surface area of GO raised from 136.3 m^2/gr up to 657.46 m^2/gr by hydrazine reduction. Increase in specific surface area indicates decrease in layer numbers. DXR Raman spectrum contribute conclusion of less layer number of ETRGO04 than ETRGO05.

Acknowledgements

Authors, thanks to Kaleseramik Çanakkale Kalebodur Seramik San. A.Ş., Fatih University BINATAM, and Tübitak MAM for their supports and contributions.

References

[1] Sathish M, Tomai T, Honma I. Graphene anchored with Fe_3O_4 nanoparticles as anode for enhanced Li-ion storage. Journal of Power Sources 2012; 217: 85-91
[2] Slonczewski JC, Weiss PR. Band structure of graphite. Phys Rev 1958;109:272.
[3] Zhang YB, Tan YW, Stormer HL, Kim P. Experimental observation of the quantum Hall effect and Berry's phase in graphene. Nature 2005;438:201.
[4] Novoselov KS, Jiang Z, Zhang Y, Morozov SV, Stormer HL, Zeitler U, et al. Room temperature quantum Hall effect in graphene. Science 2007;315:1379.
[5] Novoselov KS, Geim AK, Morozov SV, Jiang D, Katsnelson MI, Grigorieva IV, et al. Two-dimensional gas of massless Dirac fermions in graphene. Nature 2005;438:197.
[6] Novoselov KS, Geim AK, Morozov SV, Jiang D, Zhang Y, Dubonos SV, et al. Electric field effect in atomically thin carbon films. Science 2004;306:666.
[7] Balandin AA, Ghosh S, Bao W, Calizo I, Teweldebrhan D, Miao F, et al. Superior thermal conductivity of single-layer graphene. Nano Lett 2008;8:902.

[8] Lee C, Wei X, Kysar JW, Hone J. Measurement of the elastic properties and intrinsic strength of monolayer graphene.Science 2008;321:385.
[9] Wu J, Becerril HA, Bao Z, Liu Z, Chen Y, Peumans P. Organic solar cells with solution-processed graphene transparent electrodes. Appl Phys Lett 2008;92:263302.
[10] Li X, Wang X, Zhang L, Lee S, Dai H. Chemically derived, ultrasmooth graphene nanoribbon semiconductors. Science 2008;319:1229.
[11] Ritter KA, Lyding JW. The influence of edge structure on the electronic properties of graphene quantum dots and nanoribbons. Nat Mater 2009;8:235.
[12] Ubbelohde AR, Lewis LA. Graphite and its crystal compounds. London: Oxford University Press; 1960.
[13] Thompson TE, Falardeau ER, Hanlon LR. The electrical conductivity and optical reflectance of graphite–SbF5 compounds.Carbon 1977;15:39.
[14] Fuzellier H, Melin J, Herold A. Conductibilité électrique des composés lamellaires graphite–SbF5 et graphite–SbCl5. Carbon 1977;15:45.
[15] Shenderova OA, Zhirnov VV, Brenner DW. Carbon nanostructures. Crit Rev Solid State Mater Sci 2002;27:227.
[16] Krishnan A, Dujardin E, Treacy MMJ, Hugdahl J, Lynum S, Ebbesen TW. Graphitic cones and the nucleation of curved carbon surfaces. Nature 1997;388:451.
[17] Land TA, Michely T, Behm RJ, Hemminger JC, Comsa G. STM investigation of single layer graphite structures produced on Pt(111) by hydrocarbon decomposition. Surf Sci 1992;264:261.
[18] Nagashima A, Nuka K, Itoh H, Ichinokawa T, Oshima C, Otani S. Electronic states of monolayer graphite formed on TiC(111) surface. Surf Sci 1993;291:93.
[19] Forbeaux I, Themlin JM, Debever JM. Heteroepitaxial graphite on 6H–SiC(0001): interface formation through conductionband electronic structure. Phys Rev B 1998;58:16396.
[20] Berger C, Song ZM, Li TB, Li XB, Ogbazghi AY, Feng R, et al. Ultrathin epitaxial graphite: 2D electron gas properties and a route toward graphene-based nanoelectronics. J Phys Chem B 2004;108:19912.
[21] Berger C, Song Z, Li X, Wu X, Brown N, Naud Cc, et al. Electronic confinement and coherence in patterned epitaxial graphene. Science 2006;312:1191.